Analysis of the Dynamics of Liquid Aluminium: Recurrent Relation Approach

A. V. Mokshin[1,2], R. M. Yulmetyev[1,2], R. M. Khusnutdinoff[1,2] and P. Hänggi[3]

[1]*Department of Physics, Kazan State University, Kazan, Kremlyovskaya 18, 420008, Russia*
[2]*Department of Physics, Kazan State Pedagogical University, Kazan, Mezhlauk 1, 420021, Russia and*
[3]*Department of Physics, University of Augsburg,*
Augsburg, Universitätsstr. 1, D-86135 Germany
(Dated: February 4, 2008)

By use of the recurrent relation approach (RRA) we study the microscopic dynamics of liquid aluminium at $T = 973$ K and develop a theoretical model which satisfies all the corresponding sum rules. The investigation covers the inelastic features as well as the crossover of our theory into the hydrodynamical and the free-particle regimes. A comparison between our theoretical results with those following from a generalized hydrodynamical approach is also presented. In addition to this we report the results of our molecular dynamics simulations for liquid aluminium, which are also discussed and compared to experimental data. The received results reveal that (i) the microscopical dynamics of density fluctuations is defined mainly by the first four even frequency moments of the dynamic structure factor, and (ii) the inherent relation of the high-frequency collective excitations observed in experimental spectra of dynamic structure factor $S(k,\omega)$ with the two-, three- and four-particle correlations.

PACS numbers: 05.20.Jj,05.40.-a,61.20.Lc,61.20.Ne

I. INTRODUCTION

The study of dynamical processes related to atomic motions in liquid systems present an attractive research topic, both of theoretical and experimental origin. This being so, the extent of corresponding experimental knowledge about microscopic processes in liquids has continuously increased and revealed new features for various classes of liquids, which in turn call for an appropriate theoretical explanation [1]. As an intriguing example we mention the well-defined oscillatory modes observed in liquid metals occurring outside the hydrodynamic region and clearly detectable as corresponding high-frequency peaks in the experimentally relevant observable – the dynamic structure factor $S(k,\omega)$ [2, 3, 4, 5, 6]. Thus, spectra of the dynamic structure factor can display, even on microscopical spatial scales, the triple-peak form known in the hydrodynamics as the 'Brillouin triplet'.

At present various theories do exist (see, for instance, references [7, 8, 9, 10, 11, 12, 13, 14]), which suggest an explanation of the 'Brillouin triplet' evolving at the finite values of wave-number k. Their description may be found in excellent reviews [1, 15, 16], and we can assess that a great number of these theories are based on the generalization of equations of linearized hydrodynamics. However, it is necessary to point out that hydrodynamical equations are a physically correct description for a large wavelengths and time scales, where slow processes are strongly pronounced and consequently provide the significant contribution. Therefore, any wave-number and especially *time (frequency)* extension of various thermodynamic and transport quantities or the inclusion of the additional non-hydrodynamical contributions should be invoked with some care. A need to do so is particularly necessary for the description of fast processes, which are a major component of microscopic dynamics of liquids and in fact may contribute appreciably to the short-time behavior of corresponding relaxation functions (and/or into high-frequency scenario of their power spectra). The existence of finite frequency moments of $S(k,\omega)$ can serve as a peculiar criterion to test and estimate the validity of a corresponding theoretical extension [17].

In the present work we study the microscopic dynamics of liquid aluminium on the basis of the theory developed within the framework of the so-called *recurrent relation approach* (RRA) [17]. According to the RRA, the time evolution of a dynamical variable depends only on basis vectors, which span the underlying Hilbert space of the studied dynamical variable and the dimensionality of the embedding space $\mathcal{S}$ [18]. Relaxation functions and terms defining the interactions appear here as projections of dynamical variables on the corresponding orthogonal basis vectors. If the dynamical variable is a density fluctuation then the RRA allows one to obtain the corresponding relaxation function in terms of frequency moments of the dynamic structure factor.

As the specific physical system under consideration we choose the dynamics of liquid aluminium. This choice is related, foremost, to the availability of high precision data for the Inelastic X-ray Scattering (IXS) for liquid aluminium near its melting point [19]. These data are *generally* consistent with the results of molecular dynamics simulations with various models for the inter-particle potentials [20, 21, 22]. Nevertheless, it is necessary to note that the full agreement between experimental and simulation methods in characterization of dynamical features of liquid aluminium does not achieved (see p.916 of Ref. [1]).

The organization of the paper is as follows: In the next Section we present the theoretical fundamentals; in particular we review within our context the basic notions of the RRA [17, 18, 23] as these apply to the density fluctu-

ation case considered in the given work. In section III the study of various dynamical regimes and their features for the case of liquid aluminium is presented. We also report in this section details and results of our molecular dynamics simulations, which are compared with IXS-data. A resume with some concluding remarks is given in section IV.

II.   THEORETICAL FRAMEWORK

Let us consider a system of N identical classical particles of mass m evolving in the volume V. We take the density fluctuations

$$A^{(0)}(\mathbf{k}) = \frac{1}{\sqrt{N}} \sum_{j=1}^{N} e^{i\mathbf{k}\cdot\mathbf{r}_j} \qquad (1)$$

as an 'initial' dynamical variable; $\mathbf{k}$ is the wave-vector. The time evolution of $A^{(0)}(\mathbf{k})$ is defined by the Heisenberg equation

$$\frac{dA^{(0)}(\mathbf{k},t)}{dt} = i[\widehat{\mathcal{H}}, A^{(0)}(\mathbf{k},t)] = i\hat{\mathcal{L}}A^{(0)}(\mathbf{k},t), \qquad (2)$$

where $\hat{\mathcal{L}}$ is the Liouville operator, which is Hermitian, $\widehat{\mathcal{H}}$ is the Hamiltonian of the system and $[\widehat{\mathcal{H}}, \ldots]$ is the Poisson bracket. According to the RRA scheme [17, 18] the quantity $A^{(0)}(\mathbf{k},t)$ can be considered as a vector in an *a priori* chosen d-dimensional space $\mathcal{S}$, i.e.

$$A^{(0)}(k,t) = \sum_{\nu=0}^{d-1} a_\nu^{(0)}(k,t)f_\nu(k), \quad k = |\mathbf{k}| \text{ is fixed.} \quad (3)$$

Here the 'basis vectors' $f_0(k), f_1(k), ..., f_{d-1}(k)$ spanning $\mathcal{S}$ are orthogonal, i.e.,

$$(f_\nu(k), f_\mu(k)) = (f_\nu(k), f_\nu(k))\delta_{\nu\mu}, \qquad (4)$$

and are interrelated by the following recurrent relation (RR-I):

$$\begin{aligned} f_{\nu+1}(k) &= i\hat{\mathcal{L}}f_\nu(k) + \Delta_\nu(k)f_{\nu-1}(k), \quad \nu \geq 0, \\ \Delta_\nu(k) &= \frac{(f_\nu(k), f_\nu(k))}{(f_{\nu-1}(k), f_{\nu-1}(k))}, \\ f_{-1}(k) &= 0, \quad \Delta_0(k) \equiv 1. \end{aligned} \qquad (5)$$

Here $a_\nu^{(0)}(k,t)$ is the time dependent projection of $A^{(0)}(k,t)$ on the ν-th basis vector $f_\nu(k)$; the brackets $(\ldots, \ldots)$ denotes the scalar product of Kubo in the embedding space $\mathcal{S}$ [17]. Then, the relaxation function between two variables X and Y is defined by

$$(X,Y) = \frac{1}{\beta} \int_0^\beta \langle \exp(\lambda\widehat{\mathcal{H}})Y^\dagger \exp(-\lambda\widehat{\mathcal{H}})X\rangle d\lambda, \qquad (6)$$

where $X, Y \subset \mathcal{S}$, $\beta = (k_B T)^{-1}$, k_B and T are the Boltzmann constant and temperature, respectively [?]. The

angular brackets denote the average over the canonical ensemble with temperature $T = (k_B\beta)^{-1}$. Note that in the classical case ($\beta \to 0$, $\hbar \to 0$), the relaxation function proportional to the usual correlation function [17]

$$(X,Y) \equiv \langle XY^* \rangle. \qquad (7)$$

On the basis of the set of vectors $\{f_n(k)\}$ one can construct a set of dynamical variables $\{\mathbf{A}^{(n)}(k)\}$ which we need for the description of the evolution of the system, obeying

$$A^{(n)}(k,t=0) = f_n(k), \quad n = 0, 1, ..., d-1. \qquad (8)$$

The corresponding time evolution by analogy with equation (3) can be defined as

$$A^{(n)}(k,t) = \sum_{\nu=n}^{d-1} a_\nu^{(n)}(k,t)f_\nu(k). \qquad (9)$$

Note that the set of functions $a_n^{(n)}(k,t)$ (i.e. for $n = \nu$) in equations (3) and (9) are defined by projecting the dynamical variable $A^{(n)}(k,t)$ onto the corresponding basis $f_n(k)$, i.e.

$$\begin{aligned} a_n^{(n)}(k,t) &= \frac{(A^{(n)}(k,t), f_n(k))}{(f_n(k), f_n(k))} \\ &= \frac{(A^{(n)}(k,t), A^{(n)}(k,0))}{(A^{(n)}(k,0), A^{(n)}(k,0))}, \end{aligned} \qquad (10)$$

where the last equality is obtained by taking into account equation (8). So, one can easily see that these functions are *normalized*, i.e.

$$a_n^{(n)}(k,t=0) = 1. \qquad (11)$$

Here and afterwards we simplify notation whenever the quantity involves the same upper and lower index by setting: $a^{(n)}(k,t) = a_n^{(n)}(k,t)$.

The functions $a_\nu^{(n)}(k,t)$ for $\nu > n$, being defined by the projection of the vector $A^{(n)}(k,t)$ on the basis $f_\nu(k)$ with $n \neq \nu$, are related to interactions between $A^{(n)}(k)$ and $A^{(\nu)}(k)$. Further, the set $a_\nu^{(n)}(k,t)$ obeys the following properties:

$$\begin{aligned} \text{if} \quad \nu > n \quad \text{then} \quad & a_\nu^{(n)}(k,t=0) = 0, \qquad (12) \\ \text{if} \quad \nu < n \quad \text{then} \quad & a_\nu^{(n)}(k,t) \equiv 0. \end{aligned}$$

It is useful to note that the functions $a_\nu^{(n)}(k,t)$ are interrelated by the second recurrent relation (RR-II) [17], reading:

$$\Delta_{\nu+1}(k)a_{\nu+1}^{(n)}(k,t) = -\frac{da_\nu^{(n)}(k,t)}{dt} + a_{\nu-1}^{(n)}(k,t), \quad (13)$$
$$n = 0, 1, 2, \ldots d-1,$$
$$\nu = n, n+1, \ldots d-1,$$
$$\nu \geq n.$$

Thus, the set of recurrent relations (3) and (13) yield the time evolution of the dynamical variable $A^{(n)}(k)$, which occurs in the space spanned by the orthogonal basis vectors $f_n(k)$, $f_{n+1}(k)$, ...

Similar to the well-known Zwanzig-Mori formalism, these recurrent relations obey the equation [23]:

$$\frac{d}{dt}A^{(n)}(k,t) = A^{(n+1)}(k,t) - \Delta_{n+1}(k) \qquad (14)$$
$$\times \int_0^t a^{(n+1)}(k,t')A^{(n)}(k,t-t')dt',$$

which constitutes the exact reformulation of equation (2). The last equation can be rewritten in terms of the Laplace transform $\widetilde{f}(z) = \int_0^\infty e^{-zt}f(t)dt$ of the functions $a^{(n)}(t)$ as:

$$\widetilde{a}^{(n)}(k,z) = [z + \Delta_{n+1}(k)\widetilde{a}^{(n+1)}(k,z)]^{-1}. \qquad (15)$$

Then, the Laplace transform of relaxation function of the density fluctuation $\widetilde{a}^{(0)}(k,z)$ can be represented in the form of a continued fraction, i.e., [24, 25, 26]

$$\widetilde{a}^{(0)}(k,z) = \cfrac{1}{z + \cfrac{\Delta_1(k)}{z + \cfrac{\Delta_2(k)}{z + \cfrac{\Delta_3(k)}{z + \ddots}}}}. \qquad (16)$$

Thus, the time behavior of density relaxation function $a^{(0)}(k,t)$ is fully defined by the dimensionality d of the space $\mathcal{S}$ and by the corresponding set of parameters $\Delta_{n+1}(k)$ ($n = 0, 1, \ldots$). To determine $A^{(0)}(k,t)$ [and $a^{(0)}(k,t)$] it is necessary to know the whole set of the parameters $\Delta_{n+1}(k)$.

The parameters $\Delta_{n+1}(k)$ can be expressed in terms of *normalized* frequency moments of the dynamical structure factor $S(k,\omega)$ [6, 27], i.e.,

$$\omega^{(p)}(k) = (-i)^p \frac{d^p a^{(0)}(k,t)}{dt^p}\bigg|_{t=0}$$
$$= \frac{\int_{-\infty}^\infty \omega^p S(k,\omega)d\omega}{\int_{-\infty}^\infty S(k,\omega)d\omega}, \qquad (17)$$

which is related, in turn, with $a^{(0)}(k,t)$ through the Fourier transform as

$$S(k,\omega) = \frac{S(k)}{2\pi}\int_{-\infty}^\infty e^{i\omega t}a^{(0)}(k,t)dt. \qquad (18)$$

Because $S(k,\omega)$ is even function of ω for a classical system, all odd frequency moments are equal to zero. Moreover, from equations (13) and (17) and taking into ac-

count equations (11) and (12) one finds the relations

$$\omega^{(2)}(k) = \Delta_1(k), \qquad (19)$$
$$\omega^{(4)}(k) = \Delta_1^2(k) + \Delta_1(k)\Delta_2(k),$$
$$\omega^{(6)}(k) = \Delta_1(k)[\Delta_1(k) + \Delta_2(k)]^2 + \Delta_1(k)\Delta_2(k)\Delta_3(k),$$
$$\omega^{(8)}(k) = \Delta_1(k)\{[\Delta_1(k) + \Delta_2(k)]^3 + 2\Delta_2(k)\Delta_3(k)$$
$$\times[\Delta_1(k) + \Delta_2(k)] + \Delta_2(k)\Delta_3^2(k)\}$$
$$+\Delta_1(k)\Delta_2(k)\Delta_3(k)\Delta_4(k),$$
$$\omega^{(10)}(k) = \Delta_1(k)\{\Delta_1(k)[\Delta_1(k) + \Delta_2(k)]^3$$
$$+\Delta_1(k)\Delta_2(k)[\Delta_1(k) + \Delta_2(k)]$$
$$\times[\Delta_1(k) + \Delta_2(k) + \Delta_3(k)]$$
$$+\Delta_2(k)\Delta_3(k)[\Delta_1(k) + \Delta_2(k) + \Delta_3(k)]$$
$$\times[\Delta_1(k) + \Delta_2(k) + \Delta_3(k) + \Delta_4(k)]$$
$$+\Delta_2^2(k)[\Delta_1(k) + \Delta_2(k) + \Delta_3(k)]^2$$
$$+\Delta_1(k)\Delta_2(k)\Delta_3(k)[\Delta_1(k) + \Delta_2(k)]$$
$$+\Delta_2(k)\Delta_3(k)\Delta_4(k)[\Delta_1(k) + \Delta_2(k)$$
$$+\Delta_3(k) + \Delta_4(k) + \Delta_5(k)]\},$$
$$\cdots.$$

On the other hand, in the classical case, the frequency parameters $\Delta_n(k)$ can be obtained in accordance with the help of equations (5) and (7) to read:

$$\Delta_1(k) = \frac{\langle|f_1|^2\rangle}{\langle|f_0|^2\rangle} = \frac{k_BT}{m}\frac{k^2}{S(k)}, \qquad (20)$$
$$\langle|f_1|^2\rangle = \frac{k_BT}{m}k^2, \; \langle|f_0|^2\rangle = S(k),$$

By analogy with equation (20) it follows that

$$\Delta_2(k) = \frac{k_BT}{m}k^2\left(3 - \frac{1}{S(k)}\right) \qquad (21)$$
$$+ \frac{\rho}{m}\int \nabla_l^2 u(r)[1 - \exp(i\mathbf{k}\cdot\mathbf{r})]g(r)d^3\mathbf{r},$$

$$\Delta_3(k) = \frac{1}{\Delta_2(k)}\left\{15\left(\frac{k_BT}{m}k^2\right)^2 + \mathcal{F}(k)\right\}$$
$$- \frac{1}{\Delta_2(k)}[\Delta_1(k) + \Delta_2(k)]^2. \qquad (22)$$

Here, ρ denotes the number density, $S(k)$ is the static structure factor, $g(r)$ is the pair distribution function, $u(r)$ is the inter-particle potential and the suffix l denotes the component parallel to $\mathbf{k}$, whereas the term $\mathcal{F}(k)$ denotes the combination of integral expressions containing the inter-particle potential with two- and three-particle distribution functions. In the general case, the parameters $\Delta_n(k)$ at large nth order also contain the distribution functions of n, $(n-1)$, ... and $n = 2$. As a result, we can see that if the studied system is characterized by strongly pronounced potential interactions then the problem of finding the time (frequency) dependence of the dynamical variables $A^{(n)}(k)$ and/or the functions

$a^{(n)}(k,t)$ $[\widetilde{a}^{(n)}(k,z)$, see equations (15) and (16)] is reduced to the problem of truncating the chain of coupled n-th particle distribution functions [28].

III. DYNAMICAL REGIMES AND THEIR FEATURES

A. Short wavelength dynamics

Let us consider the spatio-temporal regime of a monoatomic liquid, for which one can neglect the interaction between particles. Obviously, this case corresponds to the short-time dynamics which is restricted to length scales smaller than the mean free path (i.e., the regime of high k-values). Then, the terms characterizing the strength of interaction between particles are negligible, and the static structure factor $S(k) \to 1$. Upon observing that the second (integral) term in equation (21) and $\mathcal{F}(k)$ in equation (22) are negligible one finds

$$
\begin{aligned}
\Delta_1(k) &= \frac{k_B T}{m} k^2, \\
\Delta_2(k) &= 2\Delta_1(k), \quad \Delta_3(k) = 3\Delta_1(k).
\end{aligned} \tag{23}
$$

From the first equality of equation (17) and equation (19) one derives that equations (23) represent the short-time behavior of $a^{(0)}(k,t)$ described by the Gaussian function,

$$
a^{(0)}(k,t) = \mathrm{e}^{-\Delta_1(k)t^2/2}. \tag{24}
$$

Then, from equation (13) one finds that other functions $a_n^{(0)}(k,t)$ defining interactions of density fluctuations with other dynamical variables assume the following form

$$
a_n^{(0)}(k,t) = \frac{t^n}{n!} \mathrm{e}^{-\Delta_1(k)t^2/2}, \quad n = 0,\ 1,\ \dots\ . \tag{25}
$$

Note in this case that the values of time scales determined by $\sim 1/\Delta_{n+1}(k)$ with the increase of n become smaller, and the ratio between neighboring terms converges from 2 towards 1 upon increasing n; explicitly we have

$$
\frac{\Delta_{n+2}(k)}{\Delta_{n+1}(k)} = \frac{n+2}{n+1}. \tag{26}
$$

As a result, for this regime of large k-values (opposite to the hydrodynamic limit) one can conclude that although the time scales of relaxation functions upon increasing of n also increase, they eventually become equal, i.e $\lim_{n\to\infty} \Delta_{n+2}(k)/\Delta_{n+1}(k) = 1$.

B. The fluid dynamics at intermediate wavelengths

Obviously, the simplifications used in the previous case are incorrect for microscopic spatial ranges on the scale of order of some inter-particle distances, where interaction
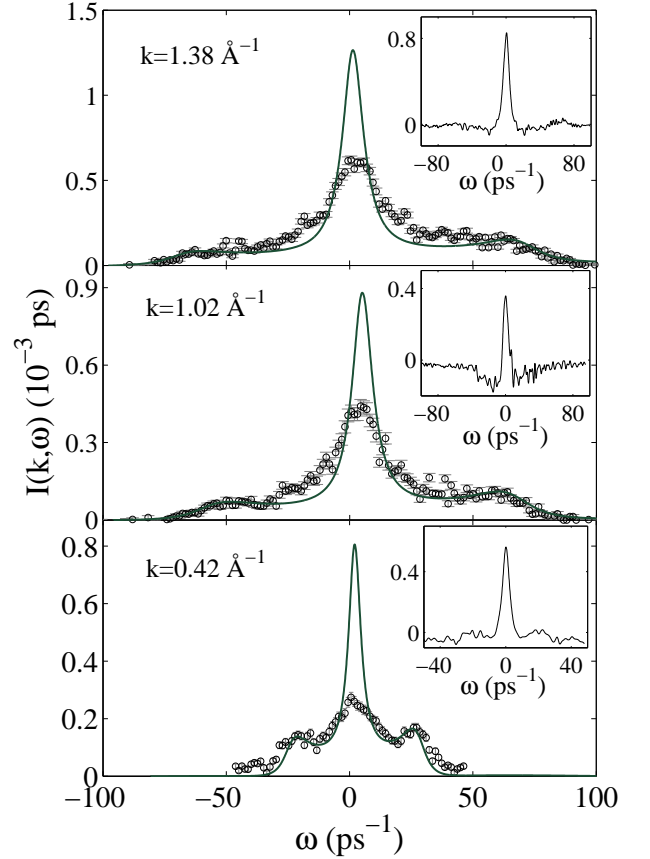

Figure 1: Main plots: the scattering intensity $I(k,\omega)$ of liquid aluminium at temperature $T = 973$ K for different wavenumbers. The solid lines present the molecular dynamics results convoluted with the experimental resolution and involving the detailed balance condition, open circles with error bars are the IXS-data of reference [19]. Insets: the difference between molecular dynamics results and interpolated experimental data at the fixed k, i.e. $I_{MD}(k,\omega) - I_{IXS}(k,\omega)$, in the units 10^{-3}ps.

between particles is considerable. This implies a more complex numerical (theoretical) evaluation of the parameters $\Delta_{n+1}(k)$, starting with the second parameter, i.e at $n = 1$ and higher.

On the other hand, the parameters $\Delta_n(k)$ can be found from molecular dynamics simulations. This is very convenient and useful tool, but it requires a priori the detailed information about the interaction of particles in the study system. According to this method, one can find the 'initial' dynamical variable $A^{(0)}(k)$ from simulation data [see equation (1)], and then receive numerically the structural parameters $\Delta_n(k)$ from RR-I [see equation (5)]. Obviously, for higher precision the carried out results should be averaged over time iterations.

We have performed such numerical analysis based on our molecular dynamics simulations for liquid aluminium

Table I: Values of the static structure factor $S(k)$, the first unnormalized frequency moment $\omega_{un}^{(2)}(k)$ and the scattering intensity at the zeroth frequency $I(k, \omega = 0)$ for liquid aluminium. IXS denotes results of reference [19] obtained from Inelastic X-ray Scattering data, whereas MD indicates outcomes of our molecular dynamics simulations.

k (nm^{-1})	$S(k)$		$\omega_{un}^{(2)}(k)$			$I(k, \omega = 0)$ (10^{-3} ps)	
	IXS	MD	$k_B T k^2/m$	IXS	MD	IXS	MD
4.2	0.010	0.029	5.288	5.294	5.443	0.250	0.805
5.4	0.013	0.032	8.741	8.732	11.010	0.320	0.826
7.8	0.016	0.034	18.239	18.241	23.170	0.350	0.837
9.0	0.020	0.037	24.283	24.192	32.758	0.390	0.844
10.2	0.025	0.037	31.190	30.925	40.351	0.425	0.896
11.4	0.027	0.045	38.961	39.021	47.598	0.434	0.910
12.6	0.030	0.050	47.595	47.631	59.238	0.520	1.174
13.8	0.036	0.059	57.092	57.137	72.048	0.601	1.253

with the particle density $n = 0.0528$ Å^{-3} at the temperature $T = 1000$ K. The interaction of $N = 4000$ particles imbedded in the cubic cell ($L = 42.32$ Å) with the periodic boundary conditions was realized using the so-called 'glue' potential [29]. The time step Δt applied in the integration of the equation of motion was 10^{-14} s. After the bringing of the system to equilibrium state, 100000 time steps were made [30, 31].

Results for the static structure factor $S(k) = \langle |f_0(k)| \rangle$ and the first *unnormalized* frequency moment $\omega_{un}^{(1)}(k) = \langle |f_1(k)| \rangle$ deduced from molecular dynamics simulations are presented in table I, where these quantities are compared with the corresponding values $S(k) = \int S(k, \omega) d\omega$ and $\omega_{un}^{(1)}(k) = \int \omega^2 S(k, \omega) d\omega$ obtained on the basis of experimental IXS-data for the dynamical structure factor $S(k, \omega)$ of liquid aluminium [19]. In this table we also give the exact theoretical prescription for the first unnormalized frequency moment $\omega_{un}^{(2)}(k) = k_B T/m$.

As can be seen, the theoretical values of $\omega_{un}^{(2)}(k)$ are in agreement with the IXS-data of reference [19] that is a quite expected, because the normalization of experimental data is performed to the first sum rules (for details, see also reference [1]), whereas the values of $\omega_{un}^{(2)}(k)$ obtained from simulations are overestimated in comparison to IXS-data for all wave-numbers. The values of the static structure factor $S(k)$ from molecular dynamics are also higher of IXS-data ($S^{MD}(k)/S^{IXS}(k) \sim 1.5 - 2.9$). As a result, the ratio between the values of the first structural parameter $\Delta_1(k) = \langle |f_1(k)| \rangle / S(k)$ from IXS-data [32] and the corresponding values from molecular dynamics simulations is $\sim 1.2 - 2.8$. The analysis performed by us reveals that the difference of high-order structural parameters obtained from IXS-data and from molecular dynamics simulations is also observed, namely, $\Delta_2^{MD}(k)/\Delta_2^{IXS}(k) \sim 2.2 - 6.7$ and $\Delta_3^{MD}(k)/\Delta_3^{IXS}(k) \sim 1.8 - 6.1$. Figure 1 compares the experimental scattering intensity $I(k, \omega)$ of liquid aluminium near melting temperature [19] and the results of molecular dynamics simulations. Although results of simulations are in a good

agreement with the IXS-data for the high-frequency region, simulation data give higher values of central peak in comparison to the experimental ones. The exact values of $I(k, \omega = 0)$ from numerical simulations and from IXS are presented in table I. On this basis, one can conclude that although the 'glue' potential of reference [29] describes correctly some equilibrium characteristics of liquid aluminium, it is unsuitable to reproduce the microscopical dynamics features of liquid aluminium, and it is unfit for finding of the structural parameters $\Delta_n(k)$.

There exists also another scheme which is based on a phenomenological estimation of the structural parameters $\Delta_n(k)$. The recent experimental IXS-data of the intensity $I(k, \omega)$ for liquid aluminium at $T = 973$ K [19] allows one to estimate the experimental frequency moments and, as a result, to identify $\Delta_{n+1}(k)$. For this procedure we employed as a fitting function the model for the classical dynamic structure factor $S(k, \omega)$ as detailed in [33], i.e.,

$$
\begin{aligned}
S(k, \omega) = {} & S(k) \frac{a \tau_1}{2} \text{sech} \left(\frac{\pi \omega \tau_1}{2} \right) \\
& + S(k) \frac{(1-a)\tau_2}{4} \left[\text{sech} \left(\frac{\pi(\omega + \omega_0)\tau_2}{2} \right) \right. \\
& \left. + \text{sech} \left(\frac{\pi(\omega - \omega_0)\tau_2}{2} \right) \right],
\end{aligned} \tag{27}
$$

with the model parameters a, τ_1, τ_2 and ω_0. It is worthwhile to note that a similar approach has been used also in [34], where the experimental $S(k, \omega)$ of liquid metals was fitted by a sum of three Gaussian functions in order to derive the first and second order memory functions numerically. However, as it was established during the fitting procedure for liquid aluminium, the model function of [33] allows one to realize a better adjustment to the experimental data (see figure 1) than the combination of Gaussian functions. As a result, after taking into account the detailed balance condition [1, 18], i.e.,

$$
S_q(k, \omega) = \frac{\hbar \omega / k_B T}{1 - e^{-\hbar \omega / k_B T}} S(k, \omega), \tag{28}
$$

Table II: Ratio of neighboring parameters $\delta_n(k) = \Delta_{n+1}(k)/\Delta_n(k)$ ($n = 1, 2, 3$ and 4) deduced according to equation (19) on the basis of experimental frequency moments for liquid aluminium at $T = 973$ K.

k (nm^{-1})	$\delta_1(k)$	$\delta_2(k)$	$\delta_3(k)$	$\delta_4(k)$
4.2	2.008	1.357	3.787	0.935
5.4	2.043	1.484	2.839	0.926
7.8	2.105	1.344	2.455	0.915
9.0	2.466	1.301	2.310	0.934
10.2	2.890	1.376	1.926	0.964
11.4	2.866	1.504	1.680	0.920
12.6	2.581	1.465	1.723	0.920
13.8	2.519	1.239	1.929	0.957

the convolution of $S_q(k,\omega)$ with the resolution function $R(k,\omega)$ was deduced to read:

$$I(k,\omega) = E(k) \int R(k, \omega - \omega') S_q(k, \omega') d\omega, \qquad (29)$$

wherein $E(k)$ denotes the form factor. The resulting function $I_f(k,\omega)$ has been adjusted to the experimental scattering function so that the the first two sum rules are obeyed identically [for $S(k)$ and $\Delta_1(k)$]. The subscript f used here for the intensity $I(k,\omega)$ denotes the fact that it is the result of a fitting procedure. The comparison of the theoretical normalized second frequency parameter from equation (20) with the obtained one from integration of the fitting dynamic structure factor $S(k,\omega)$ according to equation (17) is depicted in the main part of figure 3. Finally, the remaining parameters $\Delta_{n+1}(k)$ ($n = 1, 2, \ldots$) were deduced from $S(k,\omega)$, which yields the best fitting of $I_f(k,\omega)$ to the experimental data. The found values of the first five parameters *vs.* k are given in the inset of figure 3.

During this procedure the following features for the studied wave-number region were identified:

(i) although the frequency moments and parameters $\Delta_{n+1}(k)$ are sensitive to the form of $S(k,\omega)$, the ratio of the neighboring parameters, $\delta_n(k) = \Delta_{n+1}(k)/\Delta_n(k)$ ($n = 1, 2, \ldots$), is invariable for the various fitted func-

tions, which reproduce the experimental data within the acceptable bounds;

(ii) with increasing n for the studied wave-number region the following feature of these parameters is observed: $\Delta_{n+1}(k) > \Delta_n(k)$ ($\delta_n(k) > 1$). This feature is not valid for $n = 4$;

(iii) $\Delta_4(k)$ is *slightly larger* than $\Delta_5(k)$, $0.915 \leq \delta_4(k) \leq 0.964$ (see table II).

On this basis, we further suppose that all ratios of higher order beginning with $n = 4$ are approximately equal to 1, i.e. $\delta_n(k) \simeq 1$ for $n \geq 4$. This suffices to obtain the exact equation for dynamic structure factor. From the physical point of view, taking into account that the frequency parameters can be considered as characteristics of time scales for corresponding quantities [18, 35], such an approximation means that the average time scales of the relaxation processes related to the dynamical variables $A^{(n)}$ ($n \geq 4$) are approximately equal, i.e. $\Delta_n^{-1/2}(k) = \Delta_{n+1}^{-1/2}(k)$ for $n \geq 4$. Therefore, the time scales of 'neighbor' relaxation processes in this spatial range become equal at low levels and become strongly pronounced in comparison with the short wavelength dynamics. As a result, in the framework of the RRA one can exactly obtain the relaxation function $a_3^{(3)}(k,t)$ in the following form:

$$a^{(3)}(k,t) = \frac{1}{\sqrt{\Delta_4(k)}t} J_1(2\sqrt{\Delta_4(k)}t), \qquad (30)$$

where J_1 is the Bessel function of the first order. Further, relaxation functions of other dynamical variables and functions characterizing their interactions can be expressed by means of integral equations. However, the term of the greatest interest *a priori* is $a^{(0)}(k,t)$, the Fourier transform of which, $S(k,\omega)$, presents a experimentally measurable quantity. Therefore, from equation (30) we obtain

$$\widetilde{a}^{(3)}(k,z) = \frac{-z + [z^2 + 4\Delta_4(k)]^{1/2}}{2\Delta_4(k)}. \qquad (31)$$

Then, from equations (16) and (13) we can deduce the dynamic structure factor to read:

$$2\pi \frac{S(k,\omega)}{S(k)} = \frac{\Delta_1(k)\Delta_2(k)\Delta_3(k)}{\Delta_4(k) - \Delta_3(k)} \frac{[4\Delta_4(k) - \omega^2]^{1/2}}{\omega^6 + \mathcal{A}_1(k)\omega^4 + \mathcal{A}_2(k)\omega^2 + \mathcal{A}_3(k)}, \qquad (32)$$

$$\mathcal{A}_1(k) = \frac{\Delta_3^2(k) - \Delta_2(k)[2\Delta_4(k) - \Delta_3(k)]}{\Delta_4(k) - \Delta_3(k)} - 2\Delta_1(k),$$

$$\mathcal{A}_2(k) = \frac{\Delta_2^2(k)\Delta_4(k) - 2\Delta_1(k)\Delta_3^2(k) + \Delta_1(k)\Delta_2(k)[2\Delta_4(k) - \Delta_3(k)]}{\Delta_4(k) - \Delta_3(k)} + \Delta_1^2(k),$$

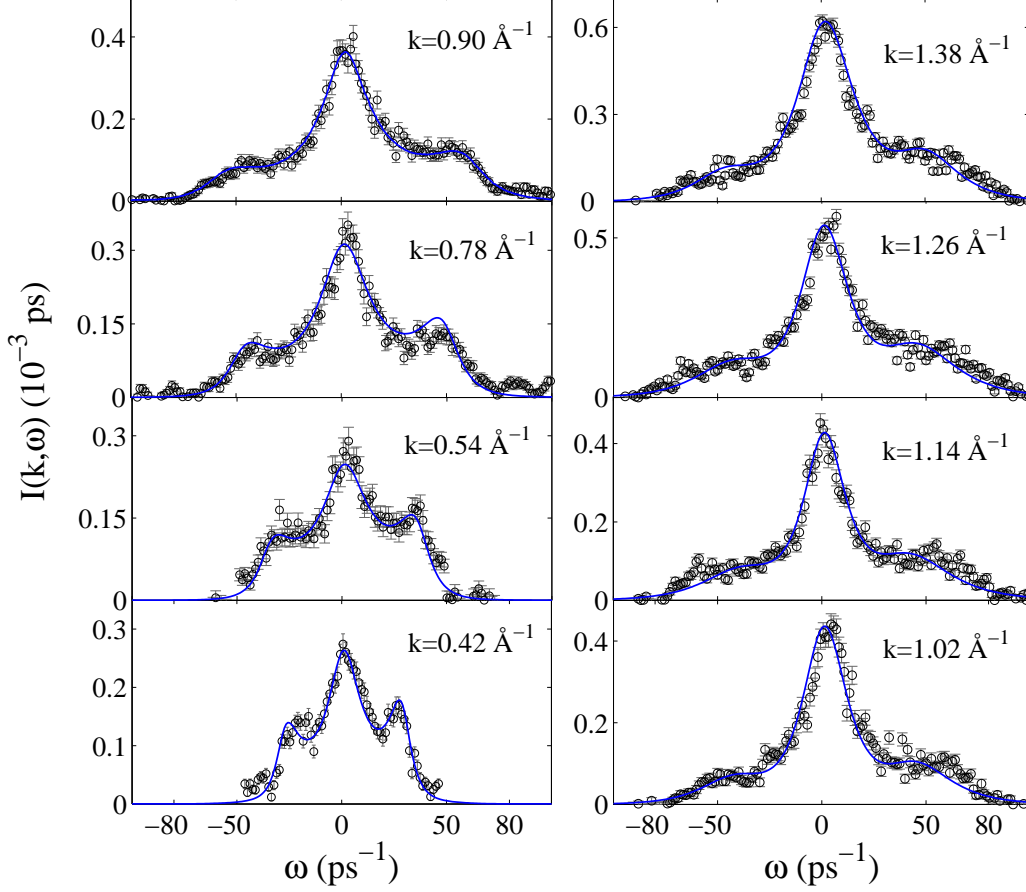$$\mathcal{A}_3(k) = \frac{\Delta_1^2(k)\Delta_3^2(k)}{\Delta_4(k) - \Delta_3(k)}.$$

Figure 2: The scattering intensity $I(k,\omega)$ of liquid aluminium at temperature $T = 973$ K. The solid lines depict the results of the theoretical model (32), whereas the open circles present the IXS-data of reference [19]. The theoretical line-shapes have been modified to account for the quantum mechanical detailed balance condition and have been broadened for the finite experimental resolution effects as described in the text.

Note that the denominator of the well known hydrodynamic dynamic structure factor $S(k,\omega)$ is also represented as the bicubic polynomial (in the variable ω) of equation (32) (see reference [36]), whereas the numerator of the hydrodynamic model contains the biquadratic polynomial. The point is that at the crossover into the hydrodynamical region (as well as into the region of free-particle motion) the equation for the dynamic structure factor (32) becomes modified. This is so because the rules of ratio for the frequency parameters are also changed. As will be presented in the next section, the so developed theory yields the correct hydrodynamical asymptotic behavior.

The comparison of the theoretical results of the dynamic structure factor $S(k,\omega)$ of liquid aluminium at $T = 973$ K according to equation (32) with data of IXS are presented with figure 2. As can be deduced from this figure, the theoretical results reproduce well the experimental data.

C. High-frequency modes

From the analysis of the experiments it is known that inelastic features of scattering spectra are pronounced in the normalized longitudinal current relaxation function

$$G_J(k,t) = \frac{(J^L(k,0), J^L(k,t))}{(J^L(k,0), J^L(k,0))}, \qquad (33)$$

which is related to the dynamic structure factor by

$$S(k)\Delta_1(k)\widetilde{G}_J(k,\omega) = \omega^2 S(k,\omega). \qquad (34)$$

The last equation can be readily obtained from

$$\Delta_1(k)G_J(k,t) = -\frac{\partial^2 a^{(0)}(k,t)}{\partial t^2}. \qquad (35)$$

The quantity $\widetilde{G}_J(k,\omega)$ possesses one minimum at $\omega = 0$ and two high-frequency maxima, being contrary to the
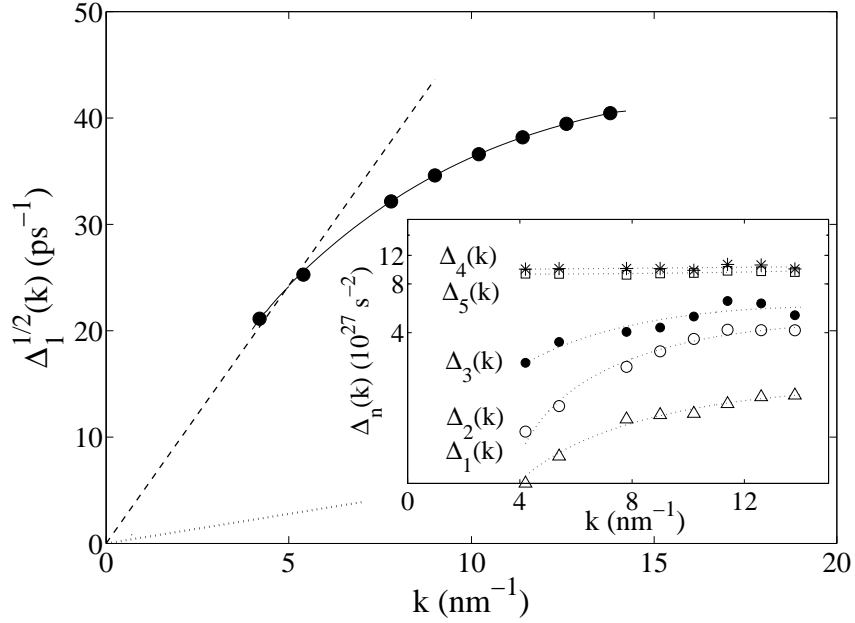
Figure 3: Main: the solid line corresponds to the theoretical results of the second frequency moment from equation (20), whereas the full circles present the values extracted by means of an integration of the resolution de-convoluted, classical $S(k,\omega)$ used to reproduce the experimental IXS-data (see in the text). The dashed and the dotted lines present the hydrodynamical limit (see equation (42a) with the isothermal sound velocity $c_0(k) = 4700$ m/s, from reference [19]) and the free-particle situations ($\Delta_1^{1/2}(k) = 1/\sqrt{\beta m}\, k$), respectively. Inset: the values of the first five parameters obtained from the frequency moments of the dynamic structure factor $S(k,\omega)$ corresponding to the best fit of $I_f(k,\omega)$ to the experimental data, as detailed in the text.

dynamic structure factor. Moreover, the side peaks in $\widetilde{G}_J(k,\omega)$ correspond to those of $S(k,\omega)$.

The inelastic features of the spectrum $\widetilde{G}_J(k,\omega)$ are defined by the solution in regard to $z = z(k)$ of the following equation (see equation (2.54) in Ref. [15]):

$$z + \frac{\Delta_1(k)}{z} + \Delta_2(k)\widetilde{a}^{(2)}(k,z) = 0, \qquad (36)$$

where $\widetilde{a}^{(2)}(k,z)$, according to the above obtained results, has the form

$$\widetilde{a}^{(2)}(k,z) = \frac{2\Delta_4(k)}{z(2\Delta_4(k) - \Delta_3(k)) + \Delta_3(k)\sqrt{z^2 + 4\Delta_4(k)}}. \qquad (37)$$

Generally, equation (36) possesses complex solutions $z = \mathrm{Re}[z(k)] + i\mathrm{Im}[z(k)]$, where $\mathrm{Im}[z(k)]$ defines the positions of the inelastic peaks in $\widetilde{G}_J(k,\omega)$, whereas $\mathrm{Re}[z(k)]$ characterizes the widths of these peaks.

Introducing for convenience the notation $\mathcal{Q}(k)$ for the ratio between the parameters $\Delta_4(k)$ and $\Delta_3(k)$, and the dimensionless quantity $\xi(k)$, with the latter characterizing the frequency region:

$$\mathcal{Q}(k) = 2\frac{\Delta_4(k)}{\Delta_3(k)} - 1, \qquad (38a)$$

$$\xi(k) = \frac{z^2}{\Delta_4(k)}, \qquad (38b)$$

the condition for the existence of side peaks in Eq. (36), can be rewritten in the following form (see Ref. [38, 39, 40]):

$$z^2 + z\Delta_2(k)\frac{1 + \mathcal{Q}(k)}{z\mathcal{Q}(k) + \sqrt{z^2 + 4\Delta_4(k)}} + \Delta_1(k) = 0. \ (39)$$

To investigate this equation further it is convenient to consider the following limiting situations. First, the region of crossover into the hydrodynamical limit can be characterized by $|\xi(k)| \ll 1$. This condition allows one to span the region of small frequencies (i.e. the large time scales). Then, the dispersion equation takes the following form:

$$z^3 + \frac{2\Delta_4^{1/2}(k)}{\mathcal{Q}(k)}z^2 + \left[\Delta_1(k) + \frac{\Delta_2(k)(1 + \mathcal{Q}(k))}{\mathcal{Q}(k)}\right]z + \frac{2\Delta_4^{1/2}(k)\Delta_1(k)}{\mathcal{Q}(k)} = 0. \qquad (40)$$

Although the exact algebraic solution of a cubic equation is feasible, it is not of much practical use here because its inherent algebraic complexity. Let us note that equation (40) is similar to the dispersion equation obtained by Mountain (see equation (15) in reference [41]). Therefore, following the convergent scheme for approximating solutions [41] one finds

$$z_{1,2}(k) = \pm i c_s k - \Gamma k^2, \qquad (41)$$

$$z_3(k) = -2\frac{\Delta_4^{1/2}(k)}{\gamma\mathcal{Q}(k)},$$

where the adiabatic sound velocity c_s, the sound damping parameter Γ, and the ratio of the specific heat at constant pressure to the specific heat at constant volume $\gamma = c_p/c_v$ read for $k \to 0$:

$$c_s = \sqrt{\gamma}c_0, \quad \lim_{k \to 0} \Delta_1(k) = c_0^2 k^2, \quad (42a)$$

$$\Gamma = \frac{\gamma - 1}{\gamma}\frac{\Delta_4^{1/2}(k)}{\mathcal{Q}(k)}, \quad (42b)$$

$$\gamma = 1 + \frac{\Delta_2(k)[1 + \mathcal{Q}(k)]}{\Delta_1(k)\mathcal{Q}(k)}, \quad (42c)$$

respectively, and $c_0(k)$ is the isothermal sound velocity. The equations (41) are the results of the hydrodynamical Landau-Placzek theory [43], and the real and imaginary parts of the first two solutions define the positions and widths of the Mandelshtam-Brillouin doublet. The approximate solutions (41) are valid, when the difference between $\Delta_4(k)$ and $\Delta_3(k)$ is sufficiently large in comparison with differences between $\Delta_3(k)$, $\Delta_2(k)$ and $\Delta_1(k)$ [44, 45]. This condition corresponds to the requirement of the Mountain approximation procedure (p.208, [41]) and is related to the divergence of the frequency parameters in the hydrodynamical limit.

If one considers the large-frequency region (regardless of k), i.e. the opposite extreme with $z^2/\Delta_4(k) \gg 1$, then here equation (39) yields

$$z_{1,2}(k) \approx \pm i\sqrt{\Delta_1(k) + \Delta_2(k)} \equiv \pm i\omega_L(k), \quad (43)$$

which corresponds to a typical 'instantaneous' solid-like response [6, 42].

As can be seen from the dispersion equation (39) both, the widths and positions of the side peaks depend on the first four parameters $\Delta_n(k)$ ($n = 1, 2, 3$ and 4). In figure 4 the square of various frequencies are compared to the square of the frequency of collective excitations, $\omega_c^2(k)$, extracted from the experimental data [19]. The results of figure 4 justify that the values of the squared frequencies of the side peaks are arranged into the intermediate region between 'hydrodynamical prescriptions' with $\gamma\Delta_1(k)$ and values $\omega_L^2(k)$ corresponding to the 'solid-like' behavior [equation (43)], while the results of our model yield the true squared frequencies of side peak, $\omega_c^2(k)$. The fact, that inelastic peaks are fully defined by the first four frequency parameters, indicates directly that the existence of side peak features in the studied region depend on both, two- and three-particle as well as four-particle interactions, which are taken into account by these parameters. Although the high-frequency motions can be considered as a remnant of solid dynamics, the large values of lifetimes of the underlying excitations (in comparison with the solid-state ones) are distinctive for the dynamics of a liquid, where two-, three- and four-particle correlations are strongly pronounced at the length scales of the order of some Angstroms.
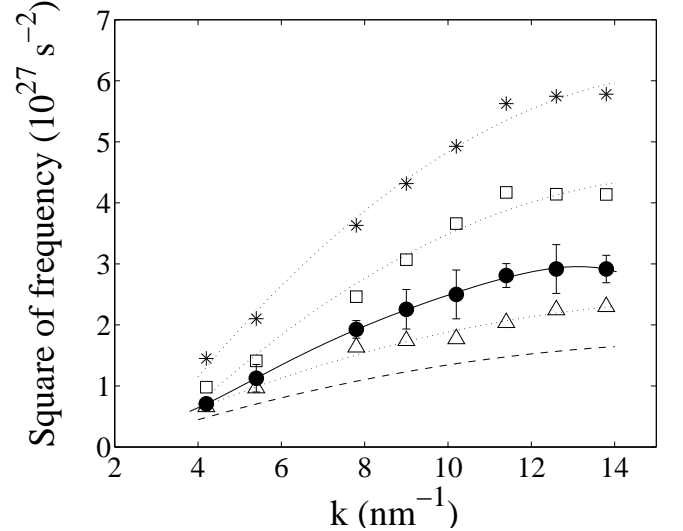

Figure 4: The short dashed line corresponds to $\Delta_1(k)$ from equation (20); the open triangles present the values of $\gamma\Delta_1(k)$, which possesses the limiting behavior $\lim_{k \to 0} \gamma\Delta_1(k) = (c_s k)^2$ and thus corresponds to the squared frequency of the Brillouin peak from hydrodynamical prescription ($\gamma = c_p/c_v = 1.4$ from references [1, 37]); the filled circles denote the squared frequency of the side peak $\omega_c^2(k)$ in the experimental IXS-spectra [19]; the solid line presents the theoretical predictions; the open squares are the values of $\Delta_2(k)$, which are obtained through the second and fourth normalized frequency moments of the resolution de-convoluted, classical dynamic structure function $S(k, \omega)$ extracted from the IXS-spectra [see equation (19)]. The squared frequency of the 'solid-like' excitations $\Delta_1(k) + \Delta_2(k) \equiv \omega_L^2(k)$ is presented by the stars.

IV. RESUME AND CONCLUDING REMARKS

As mentioned in the Introduction, the treatment of the experimental data of Inelastic Neutron Scattering (INS) and IXS experiments can be conveniently performed in the framework of generalized hydrodynamics methods. Recall that for the hydrodynamical regime the following equation holds [16]

$$\Delta_2(k)a^{(2)}(k,t) = \frac{2\eta_L k^2}{\rho m}\delta(t) + (\gamma - 1)\Delta_1(k)e^{-D_T k^2 t}, \quad (44)$$

where η_L is the longitudinal viscosity and D_T is the thermal diffusion. The last equation is obtained from a reasoning that is related to the hydrodynamical approach and is correct only for the dynamical description for large temporal and spatial scales, i.e $t \to \infty$ and $k \to 0$. However, this form of relaxation function breaks down when addressing the short-time features. From the point of view of the RRA the relaxation function corresponding to the Hermitian system can not *exactly* assume the time dependence of the form (44), because the normalized condition (11) is violated. One of the simplest generalization of the hydrodynamical approach consists in

the assumption about the extended (not instantaneous) character of the decaying viscosity term involving various elementary contributions. So, in references [1, 19] it was shown that for the correct reproduction of the experimental $S(k,\omega)$ (including the case of fluid aluminium [19]) the *three exponential decay terms* must be included at least in $a^{(2)}(k,t)$,

$$a^{(2)}(k,t) = \sum_{j=\alpha,\mu,th} \mathcal{G}_j(k)\mathrm{e}^{-t/\tau_j(k)}, \qquad (45)$$

where $\tau_\alpha(k)$ and $\tau_\mu(k)$ are the relaxation times associated with viscosity processes, whereas $\tau_{th}(k) = 1/D_T k^2$ is the relaxation time scale of thermal contribution [the second term in equation (44)], $\mathcal{G}_{\alpha,\mu,th}$ are the weights of the corresponding contributions. Although this *ansatz* also has the violation of the normalized condition (11), it can be used as a sufficiently good approximation to study THz frequency ranges (see in reference [46]).

Indeed, as can be seen from figure 3, the frequency parameter $\Delta_4(k)$ assumes the most significant values (in comparison to others) and thereby it defines the shortest time scales $2\pi/\sqrt{\Delta_4(k)} \sim 10^{-14}$s. Then the condition $|\xi(k)| \ll 1$ (see equation 38b) allows one to span the frequency (time) range $\omega < 10^{14}$s^{-1} ($t > 10^{-14}$s), which corresponds to the microscopic dynamics and is mainly available to IXS and INS. As a result, we find from equation (37) that [47]

$$\widetilde{a}^{(2)}(k,z) = \sum_j \frac{\mathcal{G}_j(k)}{z + \tau_j^{-1}(k)}, \quad \sum_j \mathcal{G}_j(k) = 1,$$
$$j = 1,\ 2,\ 3,\ 5,\ \dots, \qquad (46)$$

where $\mathcal{G}_j(k)$ and $\tau_j(k)$ are expressed in terms of $\Delta_3(k)$ and $\Delta_4(k)$ (see for details reference [46]). The given equation at $j = 3$ yields the same result as equation (45), whereas the coarse approximation at $j = 1$ corresponds to the *viscoelastic model*. Thus, we thereby justify that the expansion of the function $a^{(2)}(k,t)$ into elementary exponential contributions can be used as a good approximation in the description of the dynamics (but only) at *long* and *intermediate* time scales [9] bounded by the picosecond regime.

With this present study we have explored the dynamics of liquid aluminium at $T = 973$ K on the basis of the RRA, when the relaxation functions of the density fluctuations can be exactly extracted from the known relations between the frequency parameters $\delta_n(k) =$ $\Delta_{n+1}(k)/\Delta_n(k)$, ($n = 1, 2, \dots$). In the formulation of the RRA the parameters $\Delta_n(k)$'s constitute the structural characteristics of the embedding Hilbert space $\mathcal{S}$ of the investigated dynamical variables. As a result, the peculiarities of the dynamics depend directly on the dimension d of the space $\mathcal{S}$ and the related parameters, $\Delta_n(k)$'s. If, in particular, $\delta_n(k) \to 0$, then the realized embedding space $\mathcal{S}$ can be considered as the $(n+1)$dimensional one, and the exact solution for the relaxation function can be found [17, 18, 23]. In the opposite situation $\delta_n(k) \to \infty$, which can be observed in the hydrodynamical limit, the corresponding *exact* solution causes problems due to the divergence of the frequency parameters $\Delta_n(k)$ and $\Delta_{n+1}(k)$.

In this work we extracted phenomenologically these frequency parameters on the basis of the first five frequency moments of the experimental dynamic structure factor. The values of these five parameters increase with growing index n. A similar behavior occurs for large values of k (the free-particle case) where these parameters approach each other at large n. In the studied wavenumber region this approximate identity is observed at $n = 4$ already. The assumption that this holds as well at higher order n allows one to develop a theoretical model, which turns out to be in quantitative agreement with the experimentally observed IXS-data for liquid aluminium and which satisfies all the corresponding sum rules. We found that the first four even frequency moments appeared in the continued fraction of RRA (see equation (16)) as well as in the Zwanzig-Mori's formalism are necessary to restore the genuine microscopic dynamics of liquid aluminium. Moreover, our analysis reveals that the high-frequency features of microscopic collective dynamics in liquid aluminium depend on two-, three- and four-particle correlations. The given finding can be useful in detailed investigations of equilibrium features of fluid aluminium, at the estimation of the many-particle distribution functions, and in the studying of cluster phenomena of liquid aluminium [48] near the melting.

V. ACKNOWLEDGMENTS

[1] T. Scopigno, G. Ruocco and F. Sette, Rev. Mod. Phys **77**, 881 (2005).

[2] J. P. Boon, and S. Yip, *Molecular Hydrodynamics* (McGraw-Hill, New York, 1980).

[3] J.-L. Barrat and J.-P. Hansen, *Basic concepts for simple and complex liquids* (University Press, Cambridge, 2003).

[4] N. March, and M. Tosi, *Atomic Dynamics in Liquids* (Dover, New York, 1991).

[5] J.-P. Hansen, and I. McDonald, *Theory of Simple Liquids* (Academic, New York, 1986).

[6] U. Balucani and M. Zoppi, *Dynamics of the Liquid State* (Clarendon Press, Oxford, 1994).

[7] R. L. McGreevy and E. W. J. Mitchell, Phys. Rev. Lett. **55**, 398 (1985).

[8] C. Bruin, J. C. van Rijs, L. A. de Graaf, and I. M. de Schepper, Phys. Lett. A **110**, 40 (1988); I. M. de Schepper, E. G. D. Cohen, C. Bruin, J. C. van Rijs, W. Montfrooij, L. A. de Graaf, Phys. Rev. A **38**, 271 (1988).

[9] W. Götze, J. Phys. C **11**, A1 (1999); H.Z. Cummins, ibid. **11**, A99 (1999); L. Sjogren, Phys. Rev. A **22**, 2866 (1980); **22**, 2883 (1980); W. Götze and M.R. Mayr, Phys. Rev. E **61**, 587 (2000).

[10] I. M. de Schepper, E. G. D. Cohen, C. Bruin, J. C. van Rijs, W. Montfrooij, and L. A. de Graaf, Phys. Rev. A **38**, 271 (1988); I. M. Mryglod, I. P. Omelyan, and M. V. Tokarchuk, Mol. Phys. **84**, 235 (1995); T. Bryk and I. Mryglod, Phys. Rev. E **63**, 051202 (2001).

[11] T. Scopigno, U. Balucani, G. Ruocco, and F. Sette, Phys. Rev. E **65**, 031205 (2002).

[12] U. Bafile, E. Guarini and F. Barocchi, Phys. Rev. E **73**, 061203 (2006).

[13] L. E. Bove, F. Sacchetti, C. Petrillo, and B. Dorner, Phys. Rev. Lett. **85**, 5352 (2000); L. E. Bove, F. Sacchetti, C. Petrillo, B. Dorner, F. Formisano, and F. Barocchi, Phys. Rev. Lett. **87**, 215504 (2001); L.E. Bove, B. Dorner, C. Petrillo, F. Sacchetti and J.-B. Suck, Phys. Rev. B **68**, 024208 (2003); L.E. Bove, F. Formisano, F. Sacchetti, C. Petrillo, A. Ivanov, B. Dorner and F. Barocchi, Phys. Rev. B **71**, 014207 (2005).

[14] S. Hosokawa, Y. Kawakita, W.-C. Pilgrim, and H. Sinn, Phys. Rev. B **63**, 134205 (2001).

[15] F. Yoshida, S. Takeno, Phys. Rep. **173**, 301 (1989).

[16] J. R. D. Copley, S. W. Lovesey, Rep. Prog. Phys. **38**, 461 (1975).

[17] M. H. Lee, Phys. Rev. Lett. **51**, 1227 (1983); Phys. Rev. E **62**, 1769 (2000); Phys. Rev. E **61**, 3571 (2000).

[18] U. Balucani, M. H. Lee, and V. Tognetti, Phys. Rep. **373**, 409 (2003).

[19] T. Scopigno, U. Balucani, G. Ruocco, and F. Sette, Phys. Rev. E **63**, 011210 (2001).

[20] D. J. González, L. E. González, J. M. López, and M. J. Stott, Phys. Rev. B **65**, 184201 (2002); J. Chem. Phys. **115**, 2373 (2001).

[21] D. J. González, L. E. González, and J. M. López, J. Phys. C **13**, 7801 (2001).

[22] I. Ebbsjö, T. Kinell, and I. Waller, J. Phys. C: Solid St. Phys. **13**, 1865 (1980).

[23] M.H. Lee, Phys. Rev. E **62**, 1769 (2000), M.H. Lee, Phys. Rev. Lett. **85**, 2422 (2000).

[24] R. Zwanzig, Phys. Rev. **124**, 1338 (1961); H. Mori, Prog. Theor. Phys. **33**, 423 (1965); Prog. Theor. Phys. **34**, 399 (1965).

[25] P. Schofield, *Inelastic Scattering of Neutrons in Solids and Liquids* (IAEA, Vienna, 1961).

[26] P. Schofield, *Physics of Simple Liquids* ed. H.N.V. Temperley, J.S. Rowlinson and G.S. Rushbrooke (Amsterdam, 1968).

[27] It is convenient sometimes to use the *unnormalized* frequency moments $\omega_{un}^{(p)}(k) = \int_{-\infty}^{\infty} \omega^p S(k,\omega) d\omega$. In this definition, the zeroth frequency moment characterizes the static structure factor, i.e. $\omega_{un}^{(0)}(k) \equiv S(k)$.

[28] N. N. Bogoliubov, *Problems of Dynamic Theory in Statistical Physics* (Gostekhizdat, Moscow-Leningrad, 1946) (in Russian) [Reprinted in: Studies in statistical mechanics **1** (J. de Boer and G. E. Uhlenbeck, eds., Amsterdam, North-Holland, 1962)].

[29] F. Ercolessi, M. Parrinello and E. Tosatti, Philos. Mag. A **58**, 213 (1988); F. Ercolessi and J. B. Adams, Europhys. Lett. **26**, 583 (1994).

[30] J. J. Erpenberck and W. W. Wood, Phys. Rev. A **26**, 1648 (1982).

[31] To estimate the frequency range allowable at the molecular dynamics simulation for cell with this size [30], one can find the inverse time required for a sound wave to cross the entire periodic cell. At the length $L = 42.32$ Å and the sound velocity $c_s \simeq 4750$ m/s, it is possible to consider the frequency range $\omega \geq c_s/L$, i.e $\omega \geq 1$ ps^{-1}.

[32] The procedure of the phenomenological estimation (from IXS-data) of structural parameters will be discussed in detail below.

[33] S. Singh, and K. Tankeshwar, Phys. Rev. E **67**, 012201 (2003).

[34] K.-E. Larsson, and W. Gudowski, Phys. Rev. A **33**, 1968 (1986).

[35] A. V. Mokshin, R. M. Yulmetyev, and P. Hänggi, Phys. Rev. Lett. **95**, 200601 (2005).

[36] The comparison to result of hydrodynamical model allows one to find the following correspondence:
$\mathcal{A}_1(k) = 2[(\Gamma k^2)^2 - (c_0 k)^2] + (D_T k^2)^2$,
$\mathcal{A}_2(k) = [(\Gamma k^2)^2 + (c_0 k)^2]^2 + 2(D_T k^2)^2[(\Gamma k^2)^2 - (c_0 k)^2]$,
$\mathcal{A}_3(k) = (D_T k^2)^2[(\Gamma k^2)^2 + (c_0 k)^2]^2$.

[37] M. Inui, S. Takeda, and T. Uechi, J. Phys. Soc. Jpn. **61**, 3203 (1992)

[38] It is interesting to note that the fraction in the second term of Eq. (39) has the same form as the Laplace transform of the velocity relaxation function of the model by Rubin [39, 40] – 'impurity in the harmonic lattice', where the ratio $\Delta_4(k)/\Delta_3(k)$ corresponds to the mass ratio in the Rubin model.

[39] R. Zwanzig *Nonequilibrium statistical mechanics* (University Press, Oxford, 2001).

[40] R. J. Rubin, Phys. Rev. **131**, 964 (1963), R. J. Rubin, J. Amer. Chem. Soc. **90**, 3061 (1968); R. J. Rubin and R. Zwanzig, J. Math. Phys. **2**, 861 (1961).

[41] R.D. Mountain, Rev. Mod. Phys. **38**, 205 (1966).

[42] The same asympotic behavior is recovered from the viscoelastic model (see for example reference [6]).

[43] L. Landau and G. Placzek, Physik Z. Sowjetunion **5**, 172 (1934).

[44] In reference [45] it was found that for the case of liquid sodium the ratio $\Delta_4(k)/\Delta_3(k)$ assumes 100 and even higher at smaller, microscopic spatial scales.

[45] R. M. Yulmetyev, A. V. Mokshin, T. Scopigno, and P. Hänggi, J. Phys.: Condens. Matter **15**, 2235 (2003); R. Yulmetyev, P. Hänggi and F. Gafarov, Phys. Rev. E **62**, 6178 (2000).

[46] A. V. Mokshin, R. M. Yulmetyev, and P. Hänggi, J. Chem. Phys. **121**, 7341 (2004).

[47] Note that expansion (44) does not contradict to claims of RRA. It should be taken into account, that this expansion is suitable for finite frequency range only.

[48] E. G. Noya, J. P. K. Doye, and F. Calvo, Phys. Rev. B **73**, 125407 (2006).